ISSN 1029-9599, Physical Mesomechanics, 2019, Vol. 22, No. 1, pp. 32–41. © Pleiades Publishing, Ltd., 2019.
Russian Text © Z.P. Bažant, 2018, published in Fizicheskaya Mezomekhanika, 2018, Vol. 21, No. 6, pp. 36–44.

Dedicated to the memory of Grisha, a giant among scientists and my admired friend

A Precis of Fishnet Statistics for Tail Probability of Failure of Materials with Alternating Series and Parallel Links

Z. P. Bažant*

Northwestern University, Evanston, Illinois, 60208 USA
** e-mail: z-bazant@northwestern.edu*

Received November 15, 2018, revised November 15, 2018, accepted November 22, 2018

Abstract—During the last dozen years it has been established that the Weibull statistical theory of structural failure and strength scaling does not apply to quasibrittle materials. These are heterogeneous materials with brittle constituents and a representative volume element that is not negligible compared to the structure dimensions. A new theory of quasibrittle strength statistics in which the strength distribution is a structure size dependent graft of Gaussian and Weibull distributions has been developed. The present article gives a precis of several recent studies, conducted chiefly at the writer's home institution, in which the quasibrittle statistics has been refined to capture the statistical effect of alternating series and parallel links, which is exemplified by the material architecture of staggered platelets seen on the submicrometer scale in nacre. This architecture, which resembles a fishnet pulled diagonally, intervenes in many quasibrittle materials. The fishnet architecture is found to be advantageous for increasing the material strength at the tail of failure probability 10^{-6}, which represents the maximum tolerable risk for engineering structures and should be adopted as the basis of tail-risk design. Scaling analysis, asymptotic considerations, and cohesive fracture process zone, which were the hallmark of Barenblatt's contributions, pervade the new theory, briefly called the "fishnet statistics".

DOI: 10.1134/S1029959919010065

Keywords: probabilistic mechanics, material strength, fracture mechanics, strength scaling, size effect, nacreous materials, biomimetic materials, micromechanics of failure, nanoscale fracture, scale bridging, tolerable risk

1. INTRODUCTION

As generally accepted, engineering structures must be designed for failure probability less than 10^{-6} per lifetime [1–3], which is of the order of magnitude of the risk of death by a falling tree or lightning, and is negligible compared to the risk of death in a car accident (which is about 10^{-2} per lifetime). This requirement presents a major difficulty for the design of quasibrittle materials and structures. The quasibrittle materials are materials that have brittle constituents and a heterogeneity scale such that the representative volume element (RVE), as well as the fracture process zone (FPZ), is not negligible compared to structural dimensions.

The difficulty becomes clear from Fig. 1a, which shows the locations of the points of failure probability $P_f = 10^{-6}$ for the Gaussian (or normal) and Weibull cumulative distribution functions (cdf), for the same mean and the same coefficient of variation (CoV) (considered as 8%). Evidently, both distributions are hardly distinguishable in histograms with less than 1000 tests, yet the distances of the points of 10^{-6} from the mean differ enormously, by almost 2 : 1. Determining the 10^{-6} points is not a problem for perfectly ductile (or plastic) materials (ductile metals) or perfectly brittle materials, such as fine-grained ceramics or fatigue embrittled metals, which have a negligible representative volume element with a cumulative distribution functions

that is either Gaussian or Weibullian. Thus it suffices to calculate the mean and the CoV, which calibrates either of the two distributions completely, and the point of 10^{-6} then readily follows (Fig. 1a, bottom left). There is no problem.

However, there is a major problem for quasibrittle materials, because the point of 10^{-6} can lie anywhere between the two points marked in Fig. 1a. Besides, the location of this point depends on structure size. It can even happen (especially in the case of fishnet statistics) that, for two materials of the same CoV, the material with a higher mean strength (8% in Fig. 1b) will have much lower strength at the 10^{-6} strength probability tail (35% in Fig. 1b).

In that case the goal of material (or structure) design should not be the maximization of mean strength. Rather it should be the maximization of the strength at the 10^{-6} failure probability tail. In other words, one should pursue a tail-risk design.

Determining the failure probability of 10^{-6} experimentally, by histogram testing, is impossible. About 10^8 repetitions of the material or structure test would be needed. In the literature, there are no experimental histograms to verify failure probabilities below about 0.005. Therefore the probability distribution must be established mathematically, although the theory must be verified experimentally by checking its other predictions. Among those, the size effect is the most effective.

For mathematical determination of the material failure probability, only two theories existed until recently (Fig. 1c): the weakest-link model, which leads to Weibull distribution [4, 5], and the fiber bundle model, which leads to the Gaussian distribution [6–9]. Later it has been shown [10–12] that for quasibrittle materials the number of links in the chain must be considered finite rather than infinite, which makes Weibull distribution inapplicable to quasibrittle failure, and requires a different calculation. In 2017, a third mathematically tractable model for failure probability distribution was conceived [13, 14]—the fishnet statistics, which captures the alternation of series and parallel links as modeled by a fishnet pulled diagonally.

2. PHYSICAL BASIS OF FAILURE PROBABILITY

Where can we find the physical basis for material failure probability?—On the atomistic scale. Freudenthal's theory of critical material flaws [15] has for a long time been thought to provide the physical basis for the Weibull distribution but, on close scrutiny, it appears that it merely provides a correlation (a valid one, though). A set of hypotheses on the material scale (the power-law tail of cumulative distribution functions and the weakest link model) is replaced by another set of hypotheses on the material subscale (Frechet distribution of maximum critical flaw size, non-interacting or dilute flaws, and a point-wise fracture process zone of the flaws or microcracks).

The atomistic scale is the only one at which the probability of failure is known exactly, because the frequency equals probability. Specifically, the thermally excited atoms vibrate randomly at frequency cca 10^{14} s^{-1}, and the random jumps over the activation energy barriers cause interatomic bond breaks which eventually create nanoscale cracks (Fig. 1d, left). The highest rate of these jumps occurs under projectile impact, and assuming that at most 0.1% of the interatomic bonds get severed, the bonds are getting severed at the frequency of about 10^9 s^{-1}. Since $14 - 9 = 5$, an atom vibrates thermally about 10^5-times before a jump occurs. So (except for the chain reaction in a nuclear bomb), these jumps always represent a quasistationary process. Hence, the jump probability is equal to its frequency.

The second point important for the physical basis of failure probability is that, in similarity to the original Barenblatt's argument for the cohesive crack model [17, 18], there must be a cohesive zone on the atomistic scale (Fig. 1d, left), along which the distance between the neighboring atoms increases gradually, by many very small jumps of the cohesive crack length, until a crack opening instability is reached. The consequence is that the descending curve of the potential energy P of a nanoregion surrounding the interatomic crack cannot be smooth. Rather, an undulating potential with very many waves must be superposed on it, as shown in Fig. 1d, right [10, 11]. Therefore, the difference ΔQ between the activation energy barriers Q for the random thermal jumps forward and backward must be very small (this crucial point was missing from the classical theory of Zhurkov [19, 20], in which only a one-way barrier was considered, as if the adjacent atoms separated totally and suddenly, as if no cohesive zone existed).

The energy drop ΔQ may be related to fracture-mechanics type energy release rate at constant load P, as shown in Fig. 1d, top right. At the same time, Kramers' rule of the transition rate theory [21] can be used to

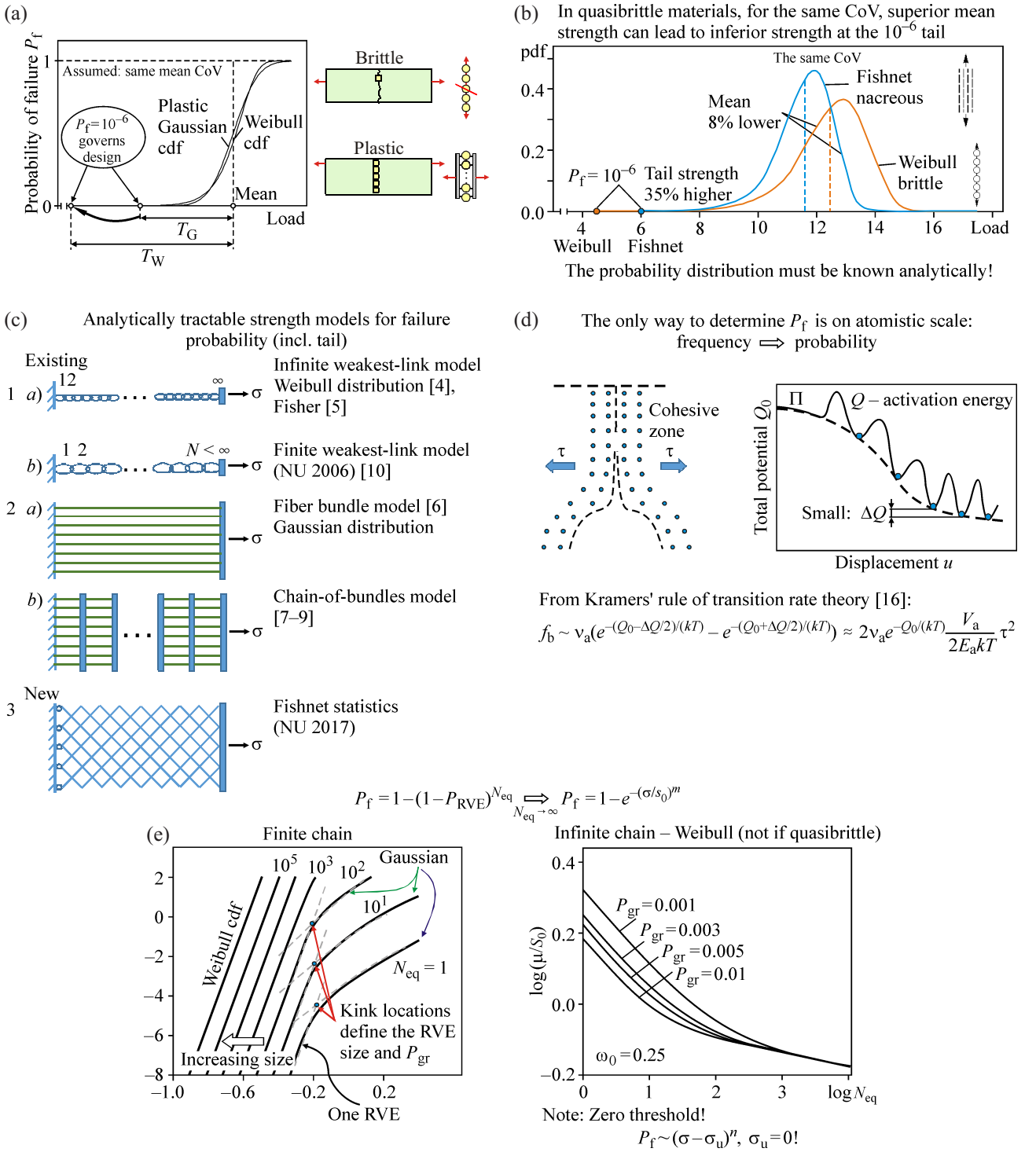

Fig. 1. The problem of distribution tail (a, b), analytically tractable models (c), physical basis of tail failure probability (d), distributions and mean size effect for finite weakest link model (*e*) (color online).

calculate the net frequency of forward jumps, i.e., the difference f_b between the frequencies of the forward and backward jumps, as shown in Fig. 1d, bottom (where T is the absolute temperature, ν_a is a constant—characteristic attempt frequency, k is the Boltzmann constant, and Q_0 is the mean activation energy barrier). Here the difference between the exponents of the two exponentials is so small that it can be replaced by the sinh-function. Then (upon examining the Péclet number of the associated Fokker–Planck equation), the

argument of the sinh is found to be in most situations so small that the sinh can be replaced by a linear function. This shows that f_b is a power law of exponent 2, in terms of the remote stress τ acting on the nanoscale region (Fig. 1d, bottom right, where V_a is the activation volume and E_a is the nanoscale Young's modulus of elasticity).

The power-law dependence of the nanoscale breakage rate, or probability, on the applied stress is an essential feature. The exponent is 2. However, on the macroscale, the power-law tail of the Weibull distribution (representing the Weibull modulus) is between 20 to 60 for all materials. How to explain this enormous increase of the power-law exponent while passing from the nanoscale to the material macroscale at the level of one representative volume element?

To explain it, the nano–macro transition, bridging the scales with fracture process zone sizes varying from 10^{-9} to 10^{-1} m in the case of concrete, has been analyzed under the simplifying hypothesis that the transition consists of some hierarchy of series and parallel connections. The series connections represent the weakest-link localizations of cracking from one scale to the next, and the parallel ones represent the conditions of compatibility of deformation at adjacent microcracks on the subscale within each fracture process zone. The analysis, which involved asymptotic expansions and recursive equations [11, 12], led to relatively simple, yet general, conclusions:

1. The power-law tail (with a zero threshold) is indestructible.

2. In series couplings, the tail exponent remains unchanged.

3. In parallel couplings, the tail exponents are additive.

4. Each parallel coupling shortens the tail reach by an order of magnitude, whereas the series coupling extends the tail reach by an order of magnitude.

5. The parallel couplings produce a cumulative distribution function with a Gaussian core.

3. STRENGTH AND LIFETIME DISTRIBUTION AT THE STRUCTURAL LEVEL

The result of the foregoing analysis is that cumulative distribution functions of strength of one representative volume element (curve for $N_{eq} = 1$ in Fig. 1e, left, plotted in Weibull scale) is Gaussian, but with a relatively abrupt transition at the low-stress tail to a power-law tail of a high exponent m such as 20 to 50. This cumulative distribution functions can be closely approximated as a Gauss–Weibull graft, with continuity of cumulative distribution function and its slope enforced at the grafting point P_g. In the typical case of positive geometry, or type 1 [12, 22], an increase of structure size D, proportional to the number N_{eq} of representative volume elements in the structure, leads to the family of cumulative distribution functions as plotted in Fig. 1a, left. The grafting point P_g moves straight up as shown, and, when the equivalent number N_{eq} of representative volume elements in the structure exceeds about 10^5, the cumulative distribution function becomes almost perfectly Weibullian (here we do not consider the energetic size effect, type 2 [18, 22–26], which is typical of most reinforced concrete structures).

But how to identify the grafting point P_g? The size effect on the mean strength μ, which can be adequately determined for each size from only 6 tests, is the answer; see Fig. 1e, where size D is measured by the equivalent number of representative volume elements N_{eq}. For large N_{eq}, the size effect is Weibullian, which is a power law of exponent m (equal to Weibull modulus) and shows up in the figures as a straight line of slope $1/m$. As the size decreases, the cumulative distribution function deviates from this line upward, and the point of deviation depends on the grafting points P_g of the cumulative distribution function, as shown in the figure for several values of P_g. It turns out that $P_g \approx 0.001$ agrees with the experimental data for concrete and other quasibrittle materials. So, the size effect tests are the way to calibrate the Gauss–Weibull cumulative distribution functions.

The deviations of quasibrittle materials from the Weibull distribution have been noticed before (for concrete, already by Weibull himself), but they have been, incorrectly, modeled by the three-parameter Weibull distribution, in which the cumulative distribution function tail is a power law of the $(\sigma - \sigma_u)^m$, where σ_u is a finite threshold, the third parameter. However, the use of a finite threshold is incorrect, for two reasons: (i) the aforementioned derivation of the Gauss–Weibull distribution can be reversed, and would indicate the Kramers' rule of transition rate theory to be invalid—an obvious contradiction; and (ii) the predicted size effect (which, habitually, has not been measured) is impossible and blatantly disagrees with the test results for large sizes [12].

In the field of ceramics it is argued that scaled tests are not needed since the devices are normally tested

at, or near, the actual size. But it is a mistake to think that scaled larger size tests are not needed. Scaling is a salient feature of the statistical failure theory and provides the key information to verify it and calibrated it. Scaled tests would have revealed that the three-parameter Weibull distribution is wrong [12].

The foregoing theory has been extended to the static and fatigue lifetimes of quasibrittle materials [27–29], including their size effect, which is much stronger than it is for monotonic loading. To that end, one needs to introduce the Charles–Evans law for static subcritical crack growth and the Paris–Erdogan law for cyclic subcritical crack growth [12], which alter the fracture geometry. Both laws have also been derived from Kramers' rule (Fig. 1a, bottom left), but a different principle had to be used. For subcritical crack growth, the tails are unimportant. The condition is that the energy dissipated in the macrofracture process zone per unit time, or per cycle, must be equal to the total energy dissipated by the fracture process zones of all the nanoscale cracks [16]. In the case of cyclic loading one must further know that the maxima and minima of cycles stress within the nanofracture process zone quickly settle on the same values which depend only the difference of the maximum and minimum of the remote applied stress but not on their values. This causes that only the amplitude of the stress intensity factor matters for the cyclic crack propagation.

The lifetime of a structure is again reached when the first representative volume element reaches its lifetime. So the weakest-link model applies, and again the number of links must be considered finite, which leads to Gauss–Weibull distribution of lifetime. Analytically, it has been shown that $m_{\mathrm{L}} = m/(n+1)$ [12, 16], where m and m_{L} are the Weibull exponents for monotonic loading and long-time or cyclic loading, and n is the exponent of the Charles–Evans or Paris–Erdogan's laws (about 10 for concrete) whose measurement takes far less time than the lifetime test. The size effect for the lifetime, whether static or cyclic, is found to be much stronger than it is for monotonic loading, which agrees with experience.

4. FISHNET STATISTICS FOR ALTERNATING SERIES AND PARALLEL LINKS

Recently it has been found [13, 14] that the well-defined submicrometer structure of nacre lends itself to a more detailed probabilistic analysis, which reveals advantageous safety aspects of nacreous material architecture and is of considerable interest for biomimetic materials. The nacre of pearle oyster or abalone is well known for its amazing strength, which is an order of magnitude higher than the strength of its main constituent, the aragonite (a type of $CaCO_3$). Fracture mechanics has been used by a number of researchers to explain the enormous mean strength deterministically [30–37]. However, biomimetic engineering applications call for probabilistic estimation of the tail failure probabilities. Do they enhance or weaken the tail strength, compared to the mean? To answer it, a new failure model, called the fishnet model, has been conceived [13, 14, 38].

In the microstructure of nacre (Fig. 2a, top and middle), almost no tension gets transmitted between the ends of two adjacent lamellae. Virtually all of the longitudinal load gets transmitted by shear through thin biopolymer layers between the bonded platelets (or lamellae). The links of the adjacent platelets are imagined as the lines connecting the lamellae centroids (Fig. 2a). The system of links looks like a fishnet pulled diagonally—hence the name (originally it was called the "tennis-net" model because the eureka moment happened to the writer, on March 9, 2017, while at the net during a doubles game, facing his student Saeed). This system can be easily simulated by a program for pin-jointed trusses (Fig. 2a, bottom left).

Consider the fishnet link strength to have failure probability $P_1(\sigma)$ described by Gauss–Weibull cumulative distribution function in which $P_{\mathrm{g}} = 0.15$. This is higher than the aforementioned value 0.001, so as to account for the fact that the bonding polymer layer is itself a structure assumed to follow a finite weakest link model. We analyze a fishnet with k rows and n columns, subjected to uniaxial applied stress σ at a rigid end plate which allows transverse sliding. The links are assumed to be brittle, i.e., to fail suddenly when their stress reaches the random strength limit. Let $P_{S_n}(\sigma)$ with $n = 0, 1, 2, 3, \ldots$ be the survival probabilities of the fishnet when exactly n links have already failed. Since these are mutually exclusive events, the survival probability of the fishnet may be calculated as indicated in Fig. 2b. It is found that normally the terms in this sum decrease rapidly and those with $n > 3$ are usually insignificant (except for large scatter of link strength).

The first term $P_{S_0}(\sigma)$ corresponds to the finite weakest-link model. The second term $P_{S_1}(\sigma)$ can be calculated according to the theorems of probability of joint and disjoint events. It has the form given in

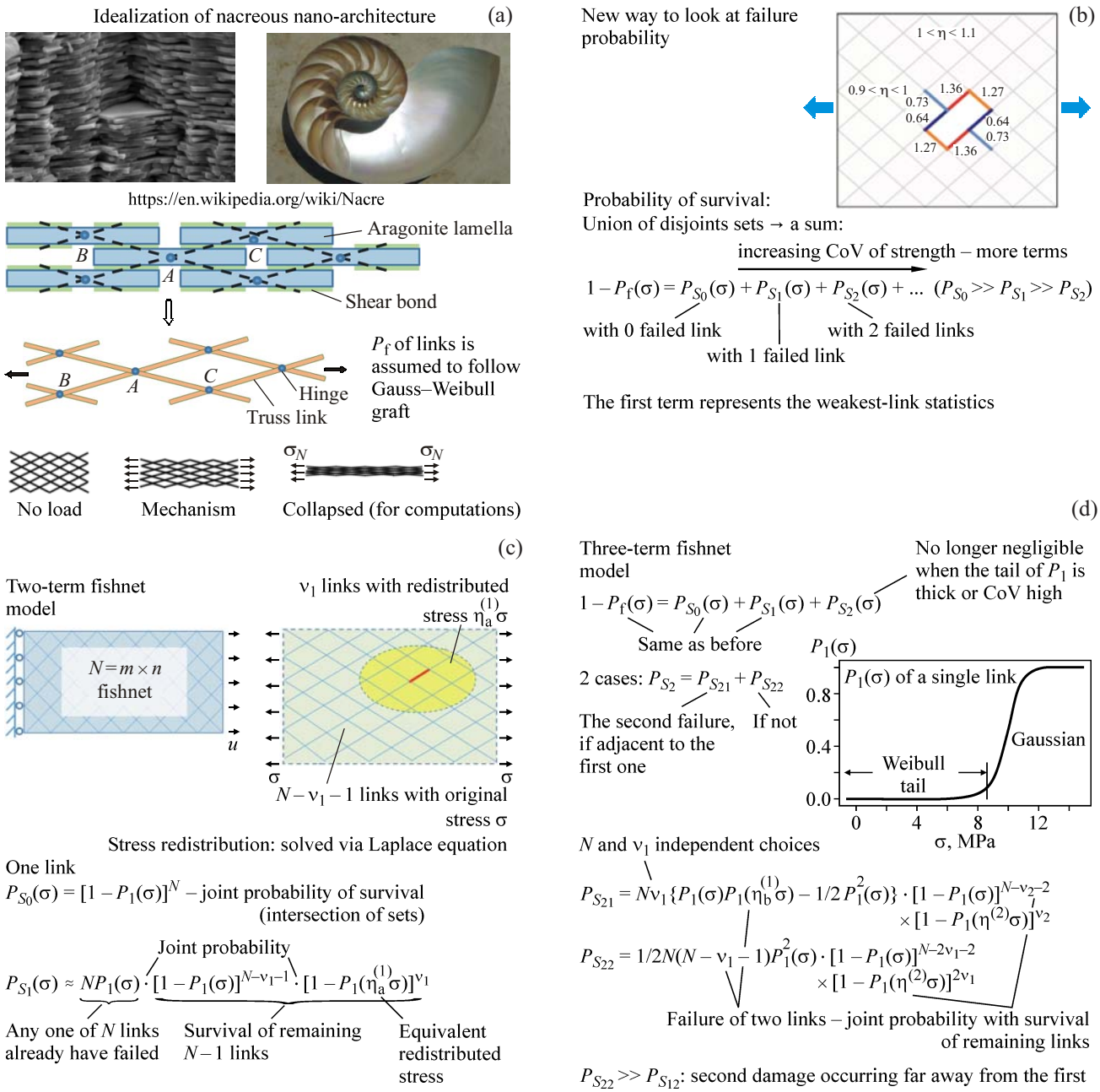

Fig. 2. Nacre and nacreous structure with alternating series and parallel connections (a), fishnet statistics (b–d) (color online).

Fig. 2c, in which λ_i is the stress redistribution factor in the *i*th link. For simplicity, this term is obtained deterministically, by solving the decay of a disturbance from the Laplace equation that represents the homogenization of the fishnet (although λ_i can be ≥1 or <1, the shielding zone with <1 can be ignored since its chance of failure is nil). The third term is more complicated but can also be calculated analytically [13, 14], by using the theorems of probability of joint and disjoint events (Fig. 2d). The fourth-term model is feasible, but too complicated.

However, for the usual coefficient of variation of the link strength, the fourth term is not needed. The analytical expressions for the first three terms seem to provide a good enough approximation for practice (Fig. 3a). The necessary number of terms is found to depend on the CoV of the scatter of link strength. When CoV → 0, the first term, representing the Weibull or Gauss–Weibull distribution, is all that is needed. With increasing CoV, the terms of the sum in Fig. 2b decrease more slowly and, for abnormally high CoV, more than three or four terms may be needed.

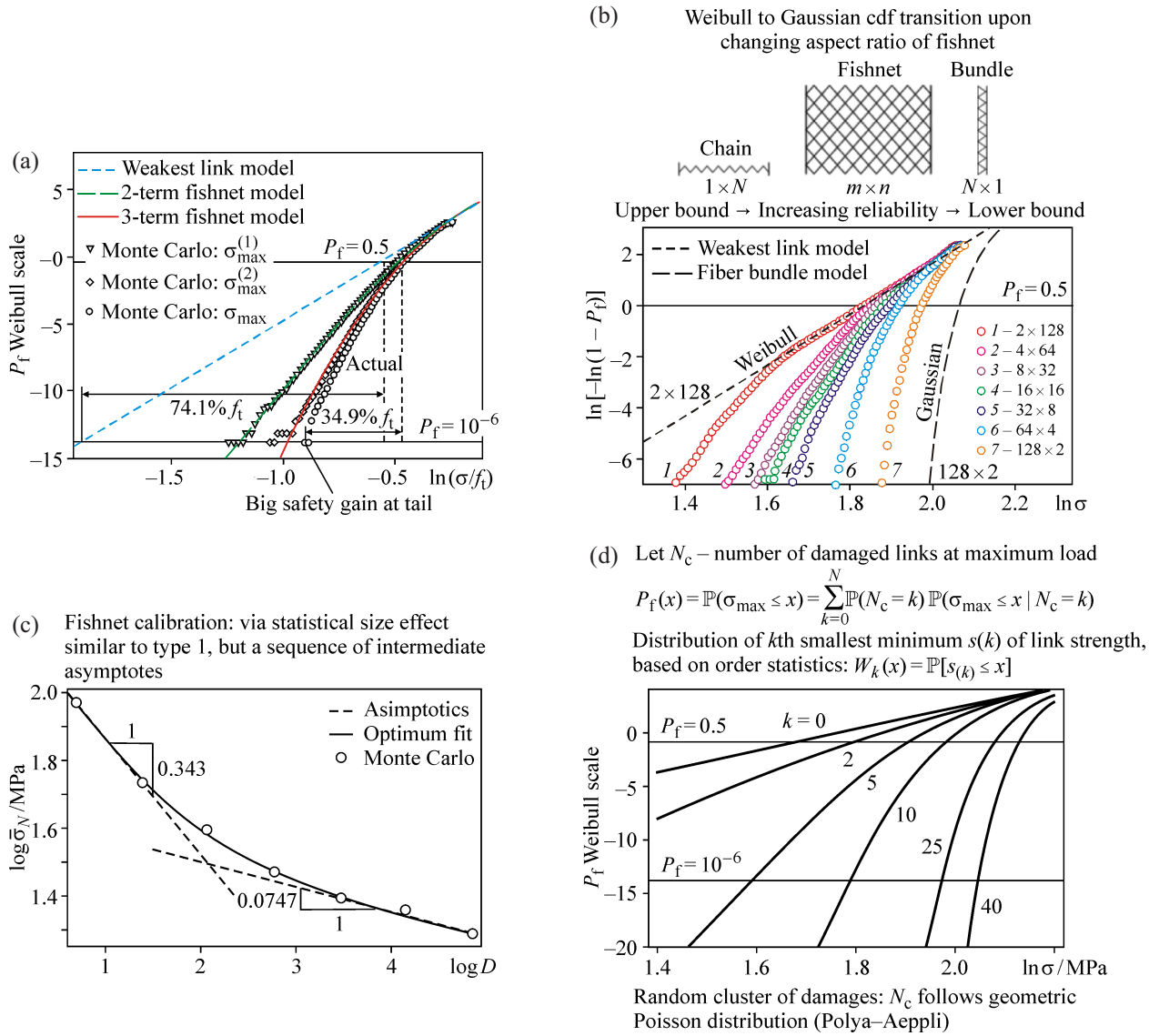

Fig. 3. Comparison with results of million Monte Carlo simulations and demonstration of safety gain at $P_f = 10^{-6}$ (a), fishnet transition from Weibull to Gaussian (or normal) distributions (b), fishnet size effect (c), distributions for progressively softening fishnet links obtained by order statistics and different minimum orders (d) (color online).

For the cases in which 0, 1 or 2 links have already failed, the distribution calculated from these equations are plotted in Weibull scale in Fig. 3a (for $k = 16$ rows and $n = 32$ columns). The circle points in this figure show the curves obtained by one million Monte Carlo simulations of the fishnet failure. About 10^4 simulations are here lumped into each data point. To simulate the curves for the two- and three-term models, the cases in which more than two or three links have failed were deleted from the histograms. The last computational histogram, with no analytical distribution to match, is the complete solution for any number of previously failed links.

From the line corresponding to probability 10^{-6}, it is evident that the fishnet model indicates an enormous additional safety advantage of nacreous material architecture, compared to the weakest link model represented in Fig. 2d by the dashed straight line (f_t in the figure is the mean strength of the links). In addition to the to transition from the Gaussian curve to the Weibull straight line of slope m occurring at high P_f, progressing further to lower P_f-values generates a gradual transition to an intermediate asymptote (in Barenblatt's sense [39, 40]) having a precisely a doubled slope $2m$. Progressing to still lower P_f-values, there is a transition to an intermediate asymptote of tripled slope, etc.

This trend continues but after the third term these transitions occur at P_f much smaller than 10^{-6}, which are of no interest. Evidently, the nacreous material architecture produces in Weibull scale a progressively steeper dipping curve, which diverges more and more from the Weibull straight line. The asymptotic slope is raised by m with each added term.

An important feature of fishnet statistics emerges when the aspect ratio (or shape) of the fishnet $k \times n$, is varied. For $k/n \to 1$, the fishnet cumulative distribution function converges to the finite weakest-link chain (or Gauss–Weibull cumulative distribution functions) and for $k/n \to \infty$ to the fiber bundle model (approaching Gaussian cumulative distribution function). The fishnet statistics can thus describe a continuous transition between these two basic classical models. This may be useful for many purposes, including the many materials that do not have the nacreous structures. In fact, quasibrittle granular materials and composites may exhibit the fishnet statistics at very low failure probabilities. Unfortunately, no existing strength histograms extend below 0.005.

An aspect of key importance is the size effect on fishnet structure strength during geometric scaling. This size effect is strong. It is of type 1 [12], but not exactly the same as it is for concrete and other randomly heterogeneous or granular quasibrittle structures. In the standard bilogarithmic plot of mean nominal strength of structure versus its characteristic size (Fig. 3c), the size effect is steeper for small sizes but approaches an asymptote with a slope much smaller than $1/m$. For the three-term fishnet, the asymptotic slope is $1/3m$.

The foregoing analysis assumes the fishnet links to be brittle or almost brittle. This means that as soon as a short crack in the bonding layer between the adjacent lamina develops, a crack would propagate along the bonding layer dynamically. However, it is possible that a crack in the bonding layer grows stably for a significant distance. In that case, the fishnet links must exhibit progressive softening, which requires a modified approach.

The key idea is to decompose the postpeak softening in the load–displacement diagram of each link into a series of small stress drops, accompanied by corresponding drops in the secant stiffness [38]. Since one small stress drop in a link cannot cause failure of the fishnet, a finite number k of stress drops is needed to cause link failure. This naturally leads to order statistics, a well-understood branch of the theory of statistics in which one seeks not the minimum of a set of independent identically distributed variables but the kth smallest minimum.

The decomposition of postpeak softening of a link into many sudden stress drops has the advantage that, due to the smallness of each stress drop, the redistribution of the stress field caused by each drop becomes minor and unimportant (whereas in Figs. 3a and 3b it is important). The order statistics is defined on top Fig. 3d, where the order $N_c = k$ must be considered as a random variable, which is known to follow the geometric Poisson distribution (or Polya–Aeppli distribution). Figure 3d shows the distributions calculated on the basis of order-statistics. What remains is to identify which distribution corresponds to the maximum load. The line of $P_f = 10^{-6}$ documents again the safety advantages of the nacreous material architecture.

5. OTHER RESULTS

Finally, it may be pointed out that, for quasibrittle materials, the Cornell reliability index and the Hasofer-Lind reliability index require a modification; see [12]. The safety design is, in structural engineering, based on the Cornell reliability index and, in a more refined form, on the Hasofer-Lind reliability index. Both can be uniquely linked to the failure probability, but have long been based on assuming the structural strength to have a Gaussian distribution. J.-L. Le recently developed important corrections to these indices, based on the finite weakest-link model and Gauss–Weibull distribution [12, ch. 11].

The Weibull distribution has long been applied to the electronic breakdown probability of dielectrics in computer chips. For the new high-k dielectrics (attaining the thickness of about 5 nm), major deviations from the Weibull distributions have been observed. The observed deviations are similar to those of the finite weakest-link chain for quasibrittle materials. A rigorous mathematical analogy with the electronic breakdown has been identified [16], and the theory adapted from strength probability has been shown to capture these deviations.

Among various civil engineering applications, one may mention the application of the finite weakest-link chain to the tragic 1959 failure of Malpasset Dam in French Alps which was the tallest and slenderest arch dam in the world. The dam failed, at the first complete filing, because of excessive slip of schist in the lateral abutment, which caused a vertical crack and type 1 failure. The analysis showed [12, 41, 42]) that the tolerable abutment displacement would now be 51% less

than what was considered in design in the 1950s, at which time the size effect in concrete was unknown.

As an application in electronics, note that the transitional Gauss–Weibull size effect has recently been demonstrated for polysilicone on the micrometer scale of MEMS [43].

6. CLOSING COMMENTS

To sum up, the main points are as follows:

(i) The only scale at which failure probability can be exactly calculated is the atomic scale, at which the probability equals the frequency.

(ii) Based on the activation energy theory of interatomic bond ruptures, the tail of the failure probability distribution on the nanoscale must be a power law of stress with exponent 2 and a zero threshold.

(iii) In the transition from the nanoscale to the macroscale of a representative volume element, the power law tail is indestructible and its exponent increases.

(iv) On the structural level, the weakest-link model of a quasibrittle structures must have a finite number of links to calibrate the strength probability distribution.

(v) The scaling, or transitional size effect, is a salient feature of quasibrittle behavior and, at the same time, the best way to calibrate the strength probability distributions.

(vi) For materials with alternating series and parallel connections in the microstructure, typified by nacre but also partially manifested in fiber composites, polycrystals, bone, concrete, etc., the tail probability may be influenced, at least to some extent, by the fishnet statistics.

(vii) Maximization of the mean material strength may, in quasibrittle materials, lead to an inferior strength at the probability tail of 10^{-6}. Therefore, the tail-risk design philosophy is more realistic.

Final note: Several important aspects of this paper draw inspirations from Grisha's perspicacious work—the atomistic cohesive crack model, the scaling arguments, the asymptotic analysis and the invocation of intermediate asymptotes.

FUNDING

The work was partially funded under ARO Grant W911NF-151-9240 to Northwestern University.

ACKNOWLEDGMENTS

Thanks are due to Wen Luo, doctoral candidate at Northwestern University, for valuable discussions.

REFERENCES

1. Duckett, K., Risk Analysis and the Acceptable Probability of Failure, *Struct. Eng.*, 2005, vol. 83(15), pp. 25–26.
2. Melchers, R.E., *Structural Reliability, Analysis and Prediction*, New York: Wiley, 1987.
3. NKB (Nordic Committee for Building Structures). Recommendation for Loading and Safety Regulations for Structural Design, *NKB Report*, 1978, no. 36.
4. Weibull, W., The Phenomenon of Rupture in Solids, *Proc. Roy. Swedish Inst. Eng. Res. Stockholm*, 1939, vol. 153, pp. 1–55.
5. Fisher, R.A. and Tippett, L.H.C., Limiting Forms of the Frequency Distribution of the Largest or Smallest Member of a Sample, *Mathematical Proceedings of the Cambridge Philosophical Society*, Cambridge University Press, 1928, vol. 24, no. 02, pp. 180–190.
6. Daniels, H.E., The Statistical Theory of the Strength of Bundles and Threads, *Proc. R. Soc. Lond. A*, 1945, vol. 183, pp. 405–435.
7. Harlow, D.G. and Phoenix, S.L., The Chain-of-Bundles Probability Model for the Strength of Fibrous Materials I: Analysis and conjectures, *J. Compos. Mater.*, 1978, vol. 12(2), pp. 195–214.
8. Harlow, D.G. and Phoenix, S.L., The Chain-of-Bundles Probability Model for the Strength of Fibrous Materials II: A Numerical Study of Convergence, *J. Compos. Mater.*, 1978, vol. 12(3), pp. 314–334.
9. Harlow, D.G. and Phoenix, S.L, Bounds on the Probability of Failure of Composite Materials, *Int. J. Fracture*, 1979, vol. 15(4), pp. 312–336.
10. Bažant, Z.P. and Pang, S.-D., Mechanics Based Statistics of Failure Risk of Quasibrittle Structures and Size Effect on Safety Factors, *Proc. Nat'l Acad. Sci. USA*, 2006, vol. 103(25), pp. 9434–9439.
11. Bažant, Z.P. and Pang, S.-D., Activation Energy Based Extreme Value Statistics and Size Effect in Brittle and Quasibrittle Fracture, *J. Mech. Phys. Solids*, 2007, vol. 55, pp. 91–134.
12. Bažant, Z.P. and Le, J.-L., *Probabilistic Mechanics of Quasibrittle Structures: Strength, Lifetime, and Size Effect*, Cambridge: Cambridge University Press, 2017.
13. Luo, Wen and Bažant, Z.P., Fishnet Model for Failure Probability Tail of Nacre-Like Imbricated Lamellar Materials, *Proc. Nati. Acad. Sci.*, 2017, vol. 114(49), pp. 12900–12905.
14. Luo, Wen and Bažant, Z.P., Fishnet Statistics for Probabilistic Strength and Scaling of Nacreous Imbricated Lamellar Materials, *J. Mech. Phys. Solids*, 2017, vol. 109, pp. 264–287 (update of Arxiv1706.01591, June 4, 2017).
15. Freudenthal, A.M., Statistical Approach to Brittle Fracture, in *Fracture: An Advanced Treatise, vol. 2*, Liebowitz, H., Ed., New York: Academic Press, 1968, pp. 591–619.

16. Bažant, Z.P., Le, J.-L., and Bažant, M.Z., Scaling of Strength and Lifetime Probability Distributions of Quasibrittle Structures Based on Atomistic Fracture Mechanics, *Proc. Nat. Acad. Sci*., 2009, vol. 106-28, pp. 11484–11489.
17. Barenblatt, G.I., The Formation of Equilibrium Cracks during Brittle Fracture, General Ideas and Hypothesis, Axially Symmetric Cracks, *Prikl. Mat. Mech*., 1959, vol. 23(3), pp. 434–444.
18. Bažant, Z.P. and Planas, J., *Fracture and Size Effect in Concrete and Other Quasibrittle Materials*, CRC Press, 1998.
19. Zhurkov, S.N., Kinetic Concept of the Strength of Solids, *Int. J. Fract. Mech*., 1965, vol. 1(4), pp. 311–323.
20. Zhurkov, S.N. and Korsukov, V.E., Atomic Mechanism of Fracture of Solid Polymer, *J. Polym. Sci*., 1974, vol. 12(2), pp. 385–398.
21. Kramers, H.A., Brownian Motion in a Field of Force and the Diffusion Model of Chemical Reaction, *Physica*, 1941, vol. 7, pp. 284–304.
22. Bažant, Z.P., Scaling Theory of Quaisbrittle Structural Failure, *Proc. Nat'l. Acad. Sci. USA*, 2004, vol. 101(37), pp. 13397–13399.
23. Bažant, Z.P., Size Effect in Blunt Fracture: Concrete, Rock, Metal, *J. Engrg. Mech. ASCE*, 1984, vol. 110(4), pp. 518–535.
24. Bažant, Z.P. and Kazemi, M.T., Determination of Fracture Energy, Process Zone Length and Brittleness Number from Size Effect, with Application to Rock and Concrete, *Int. J. Fracture*, 1990, vol. 44, pp. 111–131.
25. Bažant, Z.P., Scaling of Quasibrittle Fracture: Asymptotic Analysis, *Int. J. Fracture*, 1997, vol. 83(1), pp. 19–40.
26. Bažant, Z.P., *Scaling of Structural Strength*, London: Elsevier, 2005.
27. Bažant, Z.P. and Le, J.-L., Nano-Mechanics Based Modeling of Lifetime Distribution of Quasibrittle Structures, *J. Engrg Failure Analysis*, 2009, vol. 16, pp. 2521–2529.
28. Le, J.-L., Bažant, Z.P., and Bažant, M.Z., Unified Nano-Mechanics Based Probabilistic Theory of Quasibrittle and Brittle Structures: I. Strength, Static Crack Growth, Lifetime and Scaling, *J. Mech. Phys. Solids*, 2011, vol. 59(7), pp. 1291–1321.
29. Le, J.-L. and Bažant, Z.P., Unified Nano-Mechanics Based Probabilistic Theory of Quasibrittle and Brittle Structures: II. Fatigue Crack Growth, Lifetime and Scaling, *J. Mech. Phys. Solids*, 2011, vol. 59, pp. 1322–1337.
30. Askarinejad, S. and Rahbar, N., Toughening Mechanisms in Bioinspired Multilayered Materials, *J. Roy. Soc. Interface*, 2015, vol. 102(12), p. 20140855.
31. Chen, L., Ballarini, R., Kahn, H., and Heuer, A.H., A Bioinspired Micro-Composite Structure, *J. Mater. Res*., 2007, vol. 22, no. 1, pp. 124–131.
32. Dutta, A., Tekalur, S.A., and Miklavcic, M., Optimal Overlap Length in Staggered Architecture Composites under Dynamic Loading Conditions, *J. Mech. Phys. Solids*, 2013, vol. 61(1), pp. 145–160.
33. Dutta, A. and Tekalur, S.A., Crack Tortuousity in the Nacreous Layer—Topological Dependence and Biomimetic Design Guideline, *Int. J. Solids Struct*., 2014, vol. 51(2), p. 325335.
34. Gao, H., Ji, B., Jäger, I.L., Arzt, E., and Fratzl, P., Materials Become Insensitive to Flaws at Nanoscale: Lessons from Nature, *Proc. Nat. Acad. Sci*., 2003, vol. 100(10), pp. 5597–5600.
35. Shao, Y., Zhao, H.P., Feng, X.Q., and Gao, H., Discontinuous Crack-Bridging Model for Fracture Toughness Analysis of Nacre, *J. Mech. Phys. Solids*, 2012, vol. 60(8), pp. 1400–1419.
36. Wang, R.Z., Suo, Z., Evans, A.G., Yao, N., and Aksay, I.A., Deformation Mechanisms in Nacre, *J. Mater. Res*., 2001, vol. 16(09), pp. 2485–2493.
37. Wei, X., Filleter, T., and Espinosa, H.D., Statistical Shear Lag Model: Unraveling the Size Effect in Hierarchical Composites, *Acta Biomater*., 2015, vol. 18, pp. 206–212.
38. Luo, Wen and Bažant, Z.P., Fishnet Model with Order Statistics for Tail Probability of Failure of Nacreous Biomimetic Materials with Softening Interlaminar Links, *J. Mech. Phys. Solids*, 2018, vol. 121, pp. 281–295.
39. Barenblatt, G.I., *Scaling*, Cambridge: Cambridge University Press, 2003.
40. Barenblatt, G.I., *Similarity, Self-Similarity and Intermediate Asymptotics*, Moscow: Gidrometeoizdat, 1978; *Consultants Bureau*, New York, 1979.
41. Le, J.-L., Elias, J., and Bažant, Z.P., Computation of Probability Distribution of Strength of Quasibrittle Structures Failing at Macrocrack Initiation, *ASCE J. Engrg. Mech*., 2012, vol. 138(7), pp. 888–899.
42. Le, J.-L., Size Effect on Reliability Indices and Safety Factors of Quasibrittle Structures, *Struct. Saf*., 2015, vol. 52, pp. 20–28.
43. Le, J.-L., Ballarini, R., and Zhu, Z., Modeling of Probabilistic Failure of Polycrystalline Silicon MEMS Structures, *J. Am. Ceram. Soc*., 2015, vol. 98-6, pp. 1685–1697.